Water's role in the force-induced unfolding of ubiquitin

Jingyuan Li[a], Julio M. Fernandez[b], and B. J. Berne[a,1]

[a]Department of Chemistry, Columbia University, New York, NY 10027; and [b]Department of Biological Science, Columbia University, New York, NY 10027

Contributed by B. J. Berne, September 10, 2010 (sent for review July 13, 2010)

In atomic force spectroscopic studies of the elastomeric protein ubiquitin, the β-strands 1-5 serve as the force clamp. Simulations show how the rupture force in the force-induced unfolding depends on the kinetics of water molecule insertion into positions where they can eventually form hydrogen bonding bridges with the backbone hydrogen bonds in the force-clamp region. The intrusion of water into this region is slowed down by the hydrophobic shielding effect of carbonaceous groups on the surface residues of β-strands 1-5, which thereby regulates water insertion prior to hydrogen bond breakage. The experiments show that the unfolding of the mechanically stressed protein is nonexponential due to static disorder. Our simulations show that different numbers and/or locations of bridging water molecules give rise to a long-lived distribution of transition states and static disorder. We find that slowing down the translational (not rotational) motions of the water molecules by increasing the mass of their oxygen atoms, which leaves the force field and thereby the equilibrium structure of the solvent unchanged, increases the average rupture force; however, the early stages of the force versus time behavior are very similar for our "normal" and fictitious "heavy" water models. Finally, we construct six mutant systems to regulate the hydrophobic shielding effect of the surface residues in the force-clamp region. The mutations in the two termini of β-sheets 1-5 are found to determine a preference for different unfolding pathways and change mutant's average rupture force.

molecular dynamics simulation | single molecule spectroscopy | unfolding kinetics

There is a growing interest in the kinetic mechanisms by which elastomeric proteins unfold under force, as these proteins are involved in a wide variety of biological processes. Most elastomeric proteins (e.g., ubiquitin, I27, and fnIII) (1–3) share the common structural feature of having β-rich structures, populated by parallel β-strands. In atomic force spectroscopic studies of the elastomeric protein ubiquitin, the β-strands 1-5 serve as the force clamp under shear loading. Steered molecular dynamics (SMD) simulations (2, 4) showed that the shear loading force needs to break all four backbone hydrogen bonds (bbHBs) between the parallel β-strands 1-5 of ubiquitin in order to trigger protein unfolding (1, 5–8). In SMD simulations of I27, Lu and Schulten observed that in the early stages of the pulling process individual bbHBs occasionally break and quickly reform, due to thermal fluctuations. During these fluctuations water molecules interact with the groups of broken bbHBs, but after several picoseconds these water molecules leave the region and the bbHBs reform (9). The bbHBs in the clamp region were thought to break simultaneously right before the sheet ruptures (2, 9, 10). In our SMD studies we observe that in ubiquitin under the pulling forces the four bbHBs in the β-strands 1-5 break sequentially from either the N or C termini, accompanied by the insertion of water molecules into the broken bbHBs to form stable bridging hydrogen bonds with both bbHB partners, until the whole β-strand 1-5 ruptures. The inserted water molecules thus stabilize the broken bbHBs and facilitate the breakage of the remaining bbHBs in β-strand 1-5. This stands in contrast to the early-stage making and breaking of the bbHBs due to thermal fluctuations and the presumed simultaneous rupture of all bbHBs. In most cases the whole force-bearing β-strands rupture within 500 ps after water insertion occurs. It should also be noted that similar solvent bridge phenomena between the force-bearing β-strands were also observed in other SMD simulations of I27 (10, 11).

Because water insertion appears to be a precursor to the force-induced unfolding process, could it be that different numbers and/or locations of bridging water molecules in the clamp region give rise to a distribution of transition states for the unfolding of the mechanically stressed protein and a concomitant distribution of unfolding rate constants? Then different numbers and/or configurations of intruding water molecules would lead to a corresponding nonexponential time decay due to this static disorder. Theory and experiment suggested this in a recent paper where the distribution of the "distance to the transition state" needed to explain the experimental static disorder was found to be consistent with the distribution of the relative elongation of the end-to-end distance of protein due to the water insertion into the β-strands 1-5 determined from SMD simulation (12). To better understand the role of water, we slow down the translational motions of the water molecules in our SMD studies by increasing the mass of their oxygen atoms, thus leaving the force field and the equilibrium structure of solvent unchanged. We see that the distribution of rupture forces shifts to larger forces as the water slows down; however, the early stages of the force versus time behaviors are very similar for our "normal" and fictitious "heavy" water model. The time scale for water insertion plays a critical role in determining the transition state for unfolding and the concomitant unfolding rate constant, and the number of water molecules in proximity to the critical backbone hydrogen bond should probably be included in the definition of the reaction coordinate. Factors that control the accessibility and diffusion of water into the critical bbHBs region in the mechanically stressed proteins should be crucial to the kinetics of the unfolding process and the mechanical stability of ubiquitin.

Hydrophobicity plays an important role in such diverse systems as the self-assembly of amphiphiles (13, 14), the gating of ion channels (15), and the formation of stable protein structures (16–19). Here we focus on the effect of hydrophobic carbonaceous groups ($-CH_n-$, $n = 1, 2, 3$) on both hydrophobic and hydrophilic amino acid residues. Our SMD simulations of aqueous solutions of ubiquitin show that these hydrophobic carbonaceous groups effectively shield the bbHBs of β-strands 1-5 from water and thus kinetically hinder water from solvating and replacing these carbonyl-amid bbHBs with the hydrogen bonds to water. The pulling forces are therefore required to provide openings for the waters to gain access to these critical hydrogen bonds. Thus the hydrophobic blocking effect of these residues in the clamp region controls the kinetics of water insertion and thus the stability of ubiquitin under force loading. Therefore it would

Author contributions: J.L., J.M.F., and B.J.B. designed research; J.L. performed research; J.L. analyzed data; and J.L. and B.J.B. wrote the paper.

The authors declare no conflict of interest.

[1]To whom correspondence should be addressed. E-mail: bb8@columbia.edu.

This article contains supporting information online at www.pnas.org/lookup/suppl/doi:10.1073/pnas.1013159107/-/DCSupplemental.

be of great interest to determine how mutations changing the hydrophobic carbonaceous groups on side chains proximate to the critical hydrogen bonded region controls the behavior of water insertion, the average rupture force measuring the mechanical stability of ubiquitin, and the distribution of transition states for unfolding under force. To investigate some of these effects, we construct six mutant systems to regulate the hydrophobic shielding effect of the surface residues in the force-clamp region. The mutations in the two termini of β-sheets 1-5 are found to cause the preference for different unfolding pathways. We show that the average rupture force of mutants can be changed by choosing various numbers and locations of mutation sites and different types of target residues. Generally speaking, mutants with more surface residues mutated to glycine have smaller rupture forces than other mutants, and the rupture forces observed in mutants are also sensitive to the sizes of the hydrophobic groups on the side chains of the surface residues wrapping around the interstrand hydrogen bonds of β-strands 1-5. Clearly the hydrophobic shielding of bbHBs in the β-strands 1-5 of ubiquitin can be directly manipulated by different mutations. Water's accessibility to the bbHBs in the mechanical clamp region and concomitantly the mechanical stability of ubiquitin can then be modulated in a straightforward manner by mutation. Exploiting mutations also allows us to study by SMD simulations how the kinetics of water infiltration is related to the static disorder observed in these systems.

There have been many efforts to change the nanomechanical properties of certain proteins, by binding them to ligands (20, 21), by ion chelation (22), by inducing mutations in the hydrophobic core (23, 24), or by recombination of protein fragments from various proteins (25). It has been observed that the mutations can affect the general nanomechanical properties of proteins (21, 23, 26, 27). Very recently, the mechanical stability of Macro domain Af1521 was found to decrease by exposing the load-bearing β-sheets initially buried in the hydrophobic core (28). In agreement with our studies on ubiquitin, the authors of this work concluded that the mechanical stability of Af1521 was determined by the accessibility of water molecules to the load-bearing region of the protein, which could be modulated by altering the hydrophobic shielding of this key region (28). Much has been learned from these experiments about protein mutants. However, the change of residues can cause the protein to reorganize structurally and might change its mechanical stability in many ways. Consequently, the effects of mutations on protein mechanical stability can be attributed to multiple factors, and because of this, questions still remain (23, 29). Similar mutations in neighboring residues can cause different rupture forces (27). Investigating non-structure-changing mutations in a controlled way will further our understanding of how they can adjust the exposures of the critical bbHBs to water thereby controlling the mechanical properties. Selective mutations can allow us to probe and perhaps fine-tune the nanomechanical properties of ubiquitin in a more predictable and quantitative way and might serve as a general method for tailoring the nanomechanical properties of many other elastomeric proteins, which all have the parallel β-strands as the force-clamp region.

Results and Discussion

Effect of Water Insertion on the Unfolding. The two terminal force-bearing β-strands 1 and 5 of ubiquitin are arranged in parallel with N and C termini pointing in opposite directions. The shear topology of β-strands 1-5 can act as a mechanical clamp to resist the loading force and form the molecular basis for the mechanical stability of ubiquitin (see Fig. 1). There are five bbHBs between β-strands 1-5: Q2(CO)-E64(NH), F4(NH)-S65(CO), F4(CO)-L67(NH), K6(NH)-L67(CO), K6(CO)-L69(NH). Because the bbHB K6(CO)-L69(NH) has been found to break much earlier than the other four, the mechanical stability can be mainly attributed to the energy barriers that must be surmounted to rupture these four bbHBs.

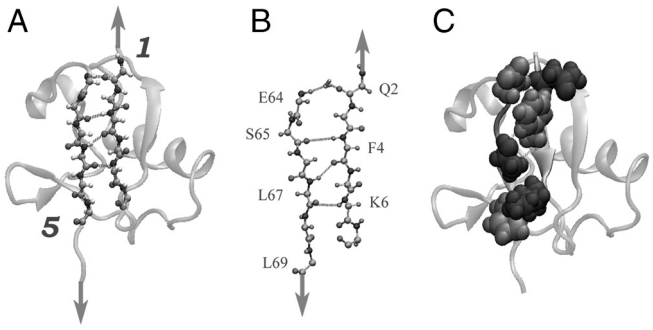

Fig. 1. The structure of ubiquitin (*A*). Cartoon of the ubiquitin protein, highlighting the location of β-strands 1 and 5 (*B*). The bbHBs and the inserted water molecules between β-strands 1 and 5 (*C*). Cartoon of the ubiquitin protein, highlighting the surface residues wrapping the bbHBs of β-strands 1 and 5 (blue and tan alternatively).

We performed 100 constant force SMD simulations (force = 667 pN) to study the mechanical unfolding process of ubiquitin. As shown in our previous paper, the four hydrogen bonds of the β-strands 1-5 do not break concurrently; they break sequentially from either the N or C terminus of β-strands 1-5. The water molecules then insert in-between the hydrogen bond acceptor (CO-) and donor (NH-) groups of the broken hydrogen bonds, forming a bridge. Fig. 2 shows that the trajectory of end-to-end length of the clamp region of ubiquitin (Q2–L69, the distance between the alpha carbon atoms of Q2 and L69) can be grouped into four stages. Stage 1 shows the initial rapid extension of the β-strands 1-5 (black); the protein then reaches at a long plateau region (stage 2, green); water molecules then insert into two separating strands forming hydrogen bond bridges between the broken backbone hydrogen bonds, which leads to further extension of β1 and β5 strands, Δx (stage 3, red); finally when all the four backbone hydrogen bonds break, the end-to-end distance increases rapidly, which indicates the unfolding of the protein (stage 4, black).

For ubiquitin in stage 3 of the unfolding process, the β-strands 1 and 5 are joined by bridging water molecules and some remaining bbHBs. When all four hydrogen bonds break, ubiquitin unfolds. Water insertion can occur from either the N or C terminus, and the number of bridging waters ranges from one to three; see Fig. 2 *B* and *C* for two examples. The number and/or configurations of bridging waters determine the relative elongation of the end-to-end distance of the β-strands 1-5 (see Fig. 2 and Fig. S1).

Even in stage 1 and stage 2, the hydrogen bonds can occasionally break and quickly reform due to thermal fluctuations (see Fig. S2). During these fluctuations water molecules can occasionally interact with the groups of broken bbHBs, but these water molecules leave the region quickly and the bbHBs reform (see Fig. 3). Similar fluctuations have been observed in SMD simulations of I27 (9). In the absence of water insertion, the hydrogen bonds always quickly reform. The bbHBs in the clamp region of I27 were thought to break simultaneously right before the protein unfolding (2, 9, 10). On the other hand, in stage 3 of ubiquitin we observe that water inserts into β-strands 1-5 by forming the hydrogen bond with both -NH and -CO groups of broken bbHB. The inserted water molecules can stay in-between the hydrogen bond group and prevent the reforming of the broken hydrogen bonds. The rupture of four hydrogen bonds in the force-clamp region can thus be further separated into multiple steps, each step corresponding to the breakage of at least one hydrogen bond. With the help of the inserted water molecules, the force does not need to rupture all four hydrogen bonds at the same time. This facilitates the unfolding process, and the inserting water

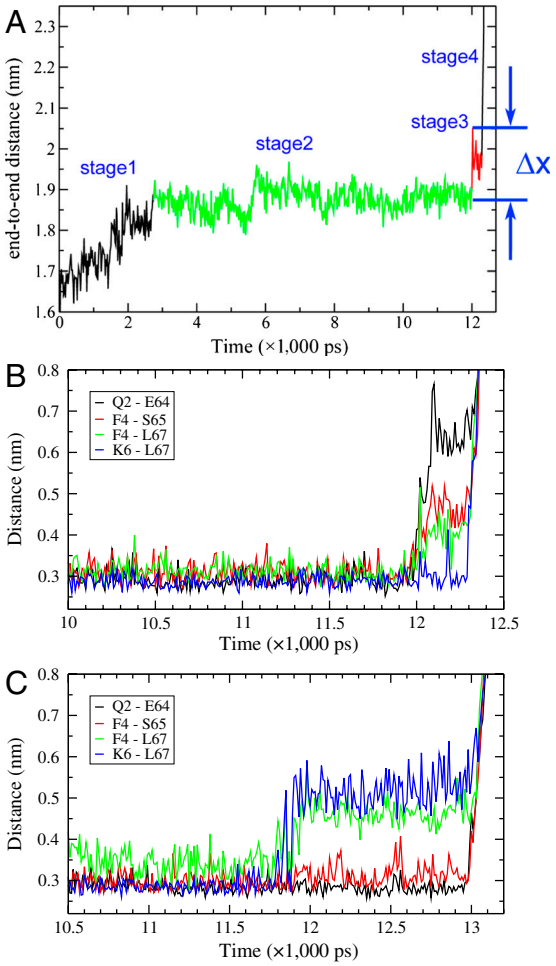

Fig. 2. Mechanical unfolding of ubiquitin in the constant-force SMD simulation (with the loading force of 667 pN) (*A*). The distance between two terminal residues Q2 and L69 of β-strands 1-5. (*Left* to *Right*) The extension curve of the end-to-end distance can be grouped into four stages: initial rapid extension (stage 1, black), long plateau region (stage 2, green), small extension due to water insertion (stage 3, red), and rapid extension for unfolding (stage 4, black) (*B*). The distances between the NH and CO groups of the four bbHBs corresponding to the trajectory given in *A*. At 12,000 ps, the distances between the NH and CO groups of the bbHBs Q2-E64 and F4-S65 increase to more than 0.45 nm as the result of water insertion at the N terminus, but water does not insert into the bbHB K6-L67 so that this H bond acts as a clamp under the loading force (*C*). In another trajectory water insertion occurs instead at the C terminus of β-strands 1-5 and the bbHBs Q2-E64 and F4-S65 serve as the clamp.

molecules play a major role in the mechanical unfolding of ubiquitin. In addition, water insertion can also enhance the exposure of the remaining bbHBs to water. As the first water molecule inserts, the rupture of the remaining bbHBs occurs quickly and cooperatively. The duration of stage 3 ranges from 300 ps to 1 ns.

In a sense water molecules catalyze the mechanical unfolding of ubiquitin. Water insertion is a key event for the mechanical-induced unfolding of protein, and we propose that ubiquitin in stage 3 is in its transition state for unfolding. We observe that once they insert, the bridging water stays between two hydrogen bond groups during the entire stage 3 up to 1 ns. We also find that in different trajectories of our SMD unfolding simulations, the numbers and/or configurations of bridging water molecules in the force-clamp β-strands 1-5 are different (Fig. 2 *B* and *C* give two of the many examples). We believe that these different embeddings of water give rise to a distribution of possible transition states for unfolding, and we never observe the interconversion of different transition states during the unfolding in our simulations. This shows that the different numbers and/or configurations of bridging water molecules leads to a "static distribution" of corresponding rate constants and thus to the experimentally observed nonexponential decay, and static disorder in the unfolding kinetics.

It is important to note that the time scale of unfolding observed in experiment (milliseconds) is much slower than in our simulations (nanoseconds) because much larger loading forces are required to reduce the central processing unit time sufficiently to make unfolding simulations feasible. Thus it could be argued that in real experiments stage 3 will be sufficiently long so that the number of bridging waters can fluctuate enough to wipe out the static disorder, but this appears not to be the case as observations show. A possible explanation is that stage 3 will still be short even for smaller loading forces. All we can say is that the simulations suggest a possible mechanism for the observed static disorder. Indeed the distribution of the distance to the transition state needed to explain the static disorder in the experiments (12) was found to be consistent with the distribution of the relative elongation (Δx) in stage 3 the end-to-end distance of protein due to the water insertion into the β-strands 1-5 occurs in stage 3 (see Fig. S1) of the unfolding process. This is shown in Fig. 2*A*.

To better understand the role of water, we performed a thought experiment in which we artificially changed the mass of water molecules by factors of 10 and 100 over the normal mass of water, leaving everything else unchanged. We find that the diffusion constants of these heavier waters decreased by factors of 3.16 and 10 correspondingly (proportional to the square root of 10 and 100 as expected) (see Fig. S3*A*). The ubiquitin was then pulled in solutions of both normal water and the fictitious "heavier" water molecules. For each system we performed 20 constant force SMD simulations with relatively larger loading force (force = 800 pN) to study the kinetics of protein unfolding, and 20 constant velocity SMD simulations (pulling rate is 0.002 nm/ps) to determine the averaged rupture forces, i.e., the relative mechanical stability of protein. In both constant force and constant velocity SMD simulations, the behavior of the extension of the proteins in heavier water was found to be similar to the proteins in normal water (with identical starting configurations) before the end-to-end length increased to 1.88 nm (corresponding to the plateau of stage 2 in Fig. 2). After this the unfolding trajectories in heavier water deviate from those of normal water. We found that water insertion was hindered by the much slower diffusion of heavier water molecules, and this makes the average rupture force larger in heavier water. In constant force SMD simulations the dwell time of water insertion, the duration of stage 2, increases from 2,800 ps to 5,000 ps (10 times heavier water) and to 11,000 ps (for 100 times heavier water, see Fig. S3*G* for representative unfolding trajectories). The kinetics of water insertion is significantly slowed down in our fictitious heavier water. Similarly, the frequency of strong attractive interactions between water and the bbHB groups in stage 2 decreases for ubiquitin in the heavier water (see Fig. S3 *H*–*J*). In constant velocity SMD simulations, the average rupture force increases from 1,200 pN to 1,420 and 1,570 pN in 10 and 100 times heavier water, which are 18% and 30% larger than in normal water. The increased rupture force in heavier water can be attributed to the fact that the water insertion is slowing down in these systems. Because the force versus time was similar for the different mass water systems up to the time water starts inserting, we infer that the initial stages do not depend on the kinetics of water but rather on the intramolecular distortions of the bbHBs. It would be very interesting to see if certain mutations that permit rapid access of water to the bbHBs eliminate the static disorder observed in the kinetics of wild type.

These results demonstrate the crucial role of water insertion in the mechanical unfolding of ubiquitin. Factors that regulate the interaction of water with the bbHBs can thus control the mechan-

ical stability of the protein. Toward this end we analyzed the interaction energy of water with NH- and CO- groups of the four bbHBs in β-strands 1-5. In the absence of a loading force, the water molecules interacted only with the NH- and CO- groups of the residues in β-strands 1-5 occasionally, and water h-bond insertion was never observed (see Fig. S4).

In the temporal evolution of the constant force SMD simulations, especially in the plateau stage 2 the groups of bbHB become more and more exposed, and interaction of the NH- and CO- groups with water gets more frequent (see Fig. 3). As the results show, the exposure of the bbHBs in the clamp region to water is an essential part of the mechanical unfolding process, especially in the plateau stage 2 where the end-to-end distance, the assumed reaction coordinate for the mechanical unfolding process, almost remains unchanged. This suggests that the end-to-end distance should not be used as the only reaction coordinate to describe the unfolding process. The relative exposure of bbHBs to water should be considered as a complementary descriptor for the mechanical unfolding process. If we could regulate the exposure of bbHBs to water we might be able to control the unfolding path.

As mentioned above, the breakage of bbHBs and water insertion occur sequentially from either N or C terminus of the β-strands 1-5. Among the 100 trajectories determined, there are 85 trajectories where water inserts starting in the N terminus. Compared to their counterparts in the C terminus, the CO (Q2) and NH (E64) groups located in the N terminus of β-strands 1-5 were found to have stronger interaction with water (see Fig. S4). A possible reason for the stronger preference for unfolding paths starting at the N terminus is that the wrapping effect of the side-chain carbonaceous groups shields the bbHB at the C terminus more than at the N terminus. It has been well accepted that the hydrophobic groups can induce the removal of water from the neighborhood of nonpolar groups. Such dehydration-based hydrophobic interactions enhance the stability of nearby intramolecular hydrogen bonds (30–32). This can be explained in terms of the competition for backbone hydrogen bonds between water molecules and the bbHB donors and acceptors. Thermal fluctuations can cause local opening and closing of backbone hydrogen bonds. When the local environment shielded the access of water, the hydrogen bond-breaking event is energetically unfavorable. The hydrophobic interaction between side-chain carbonaceous groups (CH_n, $n = 1, 2, 3$) from both hydrophobic and hydrophilic

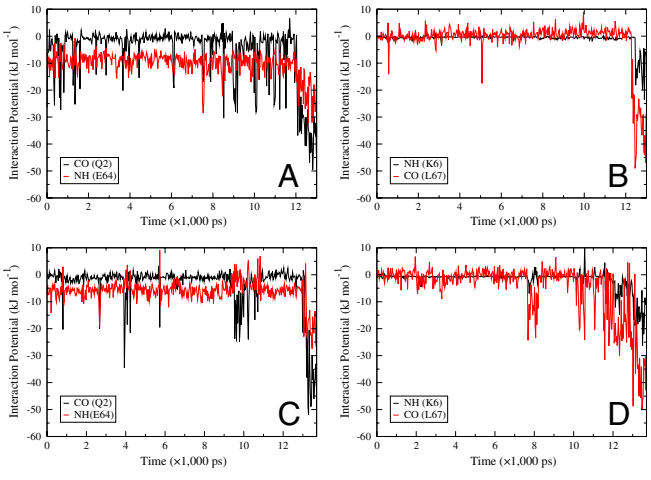

Fig. 3. The interaction potential of water with NH and CO groups of bbHBs Q2-E64 and K6-L67. Two representative simulations are chosen to show various unfolding paths. For the simulation with bbHBs breaking from N terminus, the interaction of water with CO and NH groups of Q2 and E64 become profound (*A* and *B*). For the simulation with the breakage of bbHBs starting from C terminus, the water molecules have stronger interaction with CO and NH groups of K2 and L67 become profound (*C* and *D*).

residues can effectively wrap and stabilize the nearby bbHB. In ubiquitin, the wrapping of bbHBs by the nearby hydrophobic carbonaceous groups can also inhibit water insertion during the mechanical unfolding process. There are six surface residues in β-strands 1-5 (Gln2, Phe4, Lys6, Glu64, Thr66, and His68) (shown in Fig. 1) that wrap the critical backbone hydrogen bonds and shield them from insertion of water. Compared to the Gln2 and Glu64 located in the N terminus of β-strands 1-5, Lys6 and His68 located near the C terminus have relatively more side-chain carbonaceous groups and can better shield bbHBs from water, and this can account for the preference for the unfolding path to start at the N terminus.

Effect of Mutation. In order to show that the wrapping of bbHBs can effectively guide the water insertion path, we constructed two mutant systems to reduce the shielding effect of the side-chain carbonaceous groups of residues near the N and C termini, by separately mutating two residues in the C terminus (Lys6 and His68) and N terminus (Gln2 and Glu64) to glycine, with the other residues unchanged. These mutants are denoted by *mut2C* and *mut2N*. In 50-ns simulations in the absence of force, we found that both *mut2C* and *mut2N* have stable structures as shown by the fact that the heavy atom rmsd is smaller than 3 Å, the fraction of native contacts (δ) is greater than 0.85, and the four hydrogen bonds remain intact (see Fig. S5). The mutations do not seem to change the thermostability of ubiquitin. We then used 50 constant-force SMD simulations for each mutant to study the unfolding process. The β-strands 1-5 with four bbHBs still serve as a mechanical clamp under shear loading in these simulations. We found that in *mut2C* there are 46 out of 50 trajectories in which the water insertion starts from the C terminus; thus this mutant seems to prefer unfolding paths starting at the C terminus in contrast to the wild-type unfolding that prefers to start at the N terminus. In mutant *mut2N*, all the 50 trajectories have water insertion starting at N terminus (also see Fig. S6). As shown in Fig. 4, if the sizes of the side chains of the surface residues wrapping the bbHBs of β-strands 1-5 are reduced, the bbHBs in N or C terminus of β-strands become much more exposed to water, facilitating the water interactions with the hydrogen bond groups and then water insertion. It is clear that mutations can be used to adjust the relative extent of wrapping by side-chain carbonaceous groups and thereby facilitate certain kinetic pathways for mechanical unfolding due to bbHB breakage after water insertion.

We find that more water molecules insert into the broken bbHBs of the mutants than into the wild type in stage 3 of the unfolding process, a consequence of their bbHBs being more exposed to water than are those of the wild type (see *SI Text*). In general, the more bridging water molecules that insert, the greater will be the increase in the end-to-end length. The change in end-to-end lengths due to water insertion (Δx) may relate to the distances to the transition state in mechanical unfolding (10, 12). For wild-type ubiquitin, the distribution of the end-to-end length

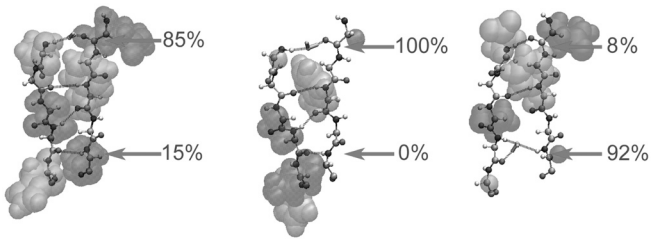

Fig. 4. The bbHBs and the inserted water molecules between β-strands 1 and 5 of wild type (*Left*), *mut2N* (*Middle*), and *mut2C* (*Right*). The red arrows indicate the percentage of the water insertion that occurs in N or C terminus of β-strands 1-5. The water molecules primarily insert from either N or C terminus in mutant systems where the side chain of surface residues wrapping the bbHBs of β-strands 1-5 (blue and tan alternatively) are reduced.

increment, Δx, has a single peak at 0.15 nm with a height of 0.45, which qualitatively agrees with the experimental fit for the distribution of the distances to the transition state in our previous paper (12). In the mutant systems, the probability of having more than one bbHB break ahead of rupture is larger than in the wild type. This results in a larger average end-to-end length increment, Δx, and a broader distribution of Δx in the mutants (see Fig. S1). This suggests that the static disorder and the concomitant nonexponential kinetics in protein unfolding might become more profound in the mutant systems.

The mutation of surface residues can not only control mechanical unfolding paths, it can also affect the general mechanical stability of mutant ubiquitins. In order to quantitatively compare the mechanical stability of the mutants with that of the wild type, 20 constant velocity SMD simulations (pulling rate is 0.002 nm/ps) were performed for *mut2C* and *mut2N* (see Fig. 5), and the averaged rupture force can be used to indicate the relative mechanical stabilities of these proteins. The average rupture force of the wild type is 1,200 pN, whereas the average rupture forces of both *mut2C* and *mut2N* decrease to 1,100 pN, 91.5% of the value of wild type (see Fig. 5*B*). The decreased mechanical stability of the mutant is due to the increased accessibility of bbHB to water.

We further investigated the dependence of nanomechanical properties of ubiquitin on side-chain wrapping in a systematic way. We constructed four additional mutant systems by replacing the three residues Phe4, Glu64, and His68 by glycine (*mut3a*), by replacing the three residues Gln2, Lys6, and Thr66 by glycine (*mut3b*), and by replacing all six of these residues by glycine (*mut6G*) or by serine (*mut6S*). Fifty-nanosecond equilibrium simulations showed that all four of these mutants were very stable. Aside from *mut6G*, the other three mutants have relatively stable bbHBs in β-strands 1-5. As for the *mut6G* system, the bbHB Q2(CO)-E64(NH) was broken after 20 ns, but the other three bbHBs remained stable (see Figs. S7 and S8). These results suggest that the reduced hydrophobic shielding effect in the force-clamp region β-strands 1-5 does not affect protein thermostability, and this might be due to the fact that there is no specific salt bridges or hydrogen bonds between the surface residues in β-strands 1-5.

These four mutants display resistance to the shear loading force to varying extents. Similar to the wild-type ubiquitin, the exposure of the bbHBs in the clamp region to water is an essential part of the mechanical unfolding process of mutants (see Fig. S9). The average rupture force of *mut3a* is 850 pN, which is 70% of the value of wild type, and the rupture force of *mut3b* is 1,050 pN, 87.5% of the value of wild type. The number of mutation sites in *mut3a* and *mut3b* is the same, whereas the relatively larger rupture force of *mut3b* might result from the better shielding effect of the side chain of Phe4. The average rupture forces of *mut6G* and *mut6S* are 700 and 1,000 pN, respectively. Even for the *mut6G* system, the shear rupture of the bbHBs in β-strands 1-5 still provides the major barrier to mechanical unfolding, whereas the average rupture force decreases to 58% of the value of the wild type. In the mutant *mut6S*, because there is only one carbonaceous group in the serine side chain, the mutation of surface residue to serine increases the blocking effect slightly compared to the glycine. This results in the relatively larger rupture force of *mut6S*. Among the mutants with the target residue glycine, the mutant with more mutation sites exhibits weaker rupture force. This also supports the conclusion about the importance of hydrophobic shielding effects.

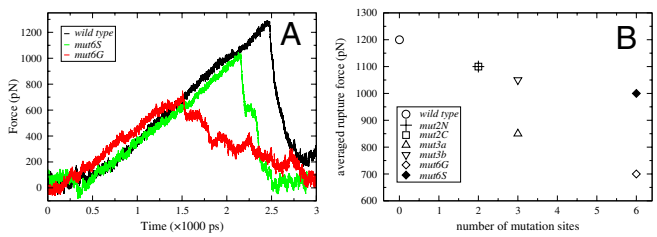

Fig. 5. Mechanical unfolding of ubiquitin in the constant-velocity SMD simulation (with the pulling rate of 0.002 nm/ps) (*A*). Three representative curves are chosen to show the different rupture forces of wild type, *mut6G*, and *mut6S* (*B*). The averaged rupture forces of wild type and six mutant systems.

There are many other mutant systems that can be constructed using various combinations of the number and location of mutation sites, together with the various target residue types. Even for the single target residue type (e.g., Gly), the number of possible combinations to construct the mutants can be 192. In this way, the nanomechanical properties of ubiquitin such as the average rupture force might be tunable within the range of from 700 to 1,200 pN, by changing the number of mutation sites, the various positions of mutation sites, and the target residue types. For example, among the mutant systems with six mutation sites, the rupture forces for the proteins should be closer to 700 pN (*mut6G*) when there are more surface residues mutated to glycine than to serine. On the other hand, the rupture forces can become larger and closer to 1,000 pN (*mut6S*) when the number of residues mutated to serine increases.

It is interesting to note that the parallel β-strands, which act as the mechanical clamp under shear loading, are the common structural feature shared by many elastomeric proteins. Thus the sensitivity to mutations should not be specific to any particular residue type in the wild-type protein. Given this, it is possible that the nanomechanical properties of many other elastomeric proteins can be tailored by mutating various surface residues in the force-clamp region.

Conclusion

In this paper, we used SMD to probe the shielding effect of the carbonaceous groups of surface residues on ubiquitin and found that they can affect water insertion during the unfolding process. Under loading forces, the bbHBs in the force-clamp region β-strands 1-5 of ubiquitin break sequentially, and water molecules facilitate this by inserting into the broken hydrogen bonds formed from liberated amine and carbonyl groups on the backbone. Water insertion stabilizes the broken bbHBs and facilitates the mechanical unfolding. The presence of water thus decreases the energy barriers that need to be surmounted to rupture these four bbHBs. To better understand the role of water, we artificially changed the mass of the water molecules by factors of 10 and 100 over the normal mass of water leaving everything else unchanged. The behavior of the extension of protein in heavier water was similar to the protein in normal water with identical starting configuration before the end-to-end length increases to 1.88 nm. Later on, the unfolding trajectories in heavier water differ from those in normal water. Water insertion was then hindered by the much slower diffusion of the heavier water molecules. On the other hand, (large) carbonaceous groups nearby can shield the bbHBs from water and slow down the process of water insertion. Shielding near the N and C termini determines whether hydrogen bond breaking starts at one or the other terminus. During the unfolding process, the loading force pulls apart the blocking groups, allowing water to get near the critical backbone hydrogen bonds, and thereby facilitating the rupture of clamp region. In this way hydrophobic shielding by carbonaceous blocking groups on the surface residues of β-strands 1-5 regulates water insertion, allowing backbone hydrogen bond breakage and subsequent force-induced unfolding of ubiquitin. Given this, we designed a series of mutant systems to manipulate the water blocking effect near the critical bbHBs by mutating the surface residues to glycine or serine, and we found that the unfolding path of protein can be regulated by the mutation and the average rupture force

required to unfold the mutants depended on the blocking capabilities of the mutations as expected from the above discussion. The nanomechanical properties of ubiquitin can thus be changed by mutations in a straightforward manner. Perhaps choosing the "right" mutations can be used to tailor the mechanical properties of other elastomeric proteins in which the β-strands also serve as the clamp region.

System and Method.

The wild-type ubiquitin protein (PDB ID code 1UBQ) was solvated in a $6.0 \times 6.0 \times 11.0$ nm^3 box of extended single point charge water model. The optimized potentials in liquid simulations all-atom force field was applied. The 50-ns simulation of equilibrium was performed to study the thermal stability of protein, and the snapshots of trajectory after 10 ns were used as the initial configurations of following SMD simulations. The equilibrium process of six mutants (*mut2N*, *mut2C*, *mut3a*, *mut3a*, *mut6G*, and *mut6G*) was performed with the similar procedure as wild-type ubiquitin.

SMD simulations with constant loading force were performed to wild-type ubiquitin, *mut2N* and *mut2C*. The C_α atoms of the terminal residues of protein were subjected to constant pulling forces of 667 pN or 800 pN in the z direction. One hundred SMD simulations were performed to study the mechanical unfolding of wild-type ubiquitin, together with 20 SMD simulations for *mut2N* and *mut2C*.

SMD simulations with constant pulling rate were performed to wild type and all six mutant systems. The C_α atoms of the terminal residues of protein were subjected to harmonic pulling potentials and were moved away from each other in the z direction with a constant velocity of 0.002 nm ps^{-1}. Fifteen simulations were performed to calculate the averaged rupture force of each protein.

The simulations were carried out with the namd2 (for equilibrium) and Gromacs 4.0.3 (for SMD simulation). Simulations were carried out with periodic boundary conditions. A time step of 2 fs was used. An N, P, T ensemble, where N is the number of atoms, P is the pressure, and T is the temperature, was simulated (see *SI Text* for more detail).

ACKNOWLEDGMENTS. We thank Drs. Ruhong Zhou and Joseph Morrone for many helpful discussions. We thank the New York Center for Computational Sciences at Brookhaven National Laboratory where most of our simulations were performed on their IBM Blue Gene/L supercomputer ("New York Blue"). This work was supported by grants from the National Institutes of Health (NIH-GM4330 to B.J.B.; NIH-HL66030 and NIH-HL61228 to J.M.F.). B.J.B. acknowledges that this work was also supported in part by the National Science Foundation through TeraGrid resources provided by National Center for Supercomputing Applications and ABE (MCA08X002).

1. Carrion-Vazquez M, et al. (2003) The mechanical stability of ubiquitin is linkage dependent. *Nat Struct Biol* 10:738–743.
2. Lu H, Schulten K (1999) Steered molecular dynamics simulation of conformational changes of immunoglobulin domain i27 interpret atomic force microscopy observations. *Chem Phys* 247:141–153.
3. Cota E, Hamill SJ, Fowler SB, Clarke J (2000) Two proteins with the same structure respond very differently to mutation: The role of plasticity in protein stability. *J Mol Biol* 302:713–725.
4. Sotomayor M, Schulten K (2007) Single-molecule experiments in vitro and in silico. *Science* 316:1144–1148.
5. Li PC, Makarov DE (2004) Ubiquitin-like protein domains show high resistance to mechanical unfolding similar to that of the i27 domain in titin: Evidence from simulations. *J Phys Chem B* 108:745–749.
6. Irback A, Mitternacht S, Mohanty S (2005) Dissecting the mechanical unfolding of ubiquitin. *Proc Natl Acad Sci USA* 102:13427–13432.
7. Kleiner A, Shakhnovich E (2007) The mechanical unfolding of ubiquitin through all-atom Monte Carlo simulation with a go-type potential. *Biophys J* 92:2054–2061.
8. Cieplaka M, Marszalek PE (2005) Mechanical unfolding of ubiquitin molecules. *J Chem Phys* 123:194903.
9. Lu H, Schulten K (2000) The key event in force-induced unfolding of titins immunoglobulin domains. *Biophys J* 79:51–65.
10. Dougan L, Feng G, Lu H, Fernandez JM (2008) Solvent molecules bridge the mechanical unfolding transition state of a protein. *Proc Natl Acad Sci USA* 105:3185–3190.
11. Pabón G, Amzel LM (2006) Mechanism of titin unfolding by force: Insight from quasi-equilibrium molecular dynamics calculations. *Biophys J* 91:467–472.
12. Kuo TL, et al. (2010) The kinetics of ubiquitin unfolding exhibits the feature of static disorder captured by single-molecule experiments. *Proc Natl Acad Sci USA* 107:11336–11340.
13. Tanford C (1972) Hydrophobic free energy, micelle formation and the association of proteins with amphiphiles. *J Mol Biol* 67:59–74.
14. Israelachvili JN, Mitchell DJ, Ninham BW (1976) A theory of self-assembly of hydrocarbon amphiphiles into micelles and bilayers. *J Chem Soc Faraday Trans 2* 72:1525–1568.
15. Anishkin A, Sukharev S (2004) Water dynamics and dewetting transitions in the small mechanosensitive channel MscS. *Biophys J* 86:2883–2895.
16. Zhou R, Huang X, Margulius CJ, Berne BJ (2004) Hydrophobic collapse in multi-domain protein folding. *Science* 305:1605–1609.
17. Liu P, Huang X, Zhou R, Berne BJ (2005) Drying and hydrophobic collapse of melittin tetramer. *Nature* 437:159–162.
18. Levy Y, Onuchic JN (2006) Water mediation in protein folding and molecular recognition. *Ann Rev Bioph Biom* 35:389–415.
19. Papoian GA, Ulander J, Wolynes PG (2003) Role of water mediated interactions in protein-protein recognition landscapes. *J Am Chem Soc* 125:9170–9178.
20. Puchner EM, et al. (2008) Mechanoenzymatics of titin kinase. *Proc Natl Acad Sci USA* 105:13385–13390.
21. Cao Y, Li H (2008) Engineered elastomeric proteins with dual elasticity can be controlled by a molecular regulator. *Nat Nanotechnol* 3:512–516.
22. Cao Y, Yoo T, Li H (2008) Single molecule force spectroscopy reveals engineered metal chelation is a general approach to enhance mechanical stability of proteins. *Proc Natl Acad Sci USA* 105:11152–11157.
23. Craig D, Gao M, Schulten K, Vogel V (2004) Tuning the mechanical stability of fibronectin type III modules through sequence variations. *Structure* 12:21–30.
24. Williams PM, et al. (2003) Hidden complexity in the mechanical properties of titin. *Nature* 422:446–449.
25. Sharma D, Cao Y, Li H (2006) Engineering proteins with novel mechanical properties by recombination of protein fragments. *Angew Chem Int Edit* 45:5633–5638.
26. Marszalek PE, et al. (1999) Mechanical unfolding intermediates in titin modules. *Nature* 402:100–103.
27. Li H, Carrion-Vazquez M, Oberhauser AF, Marszalek PE, Fernandez JM (2000) Point mutations alter the mechanical stability of immunoglobulin modules. *Nat Struct Biol* 7:1117–1120.
28. Guzman DL, Randall A, Baldi P, Guan Z (2010) Computational and single-molecule force studies of a macro domain protein reveal a key molecular determinant for mechanical stability. *Proc Natl Acad Sci USA* 107:1989–1994.
29. Ng SP, Clarke J (2007) Experiments suggest that simulations may overestimate electrostatic contributions to the mechanical stability of a fibronectin type III domain. *J Mol Biol* 371:851–854.
30. Garcia AE, Sanbonmatsu KY (2002) Alpha-helical stabilization by side chain shielding of backbone hydrogen bonds. *Proc Natl Acad Sci USA* 99:2782–2787.
31. Vila JA, Ripoll DR, Scheraga HA (2000) Physical reasons for the unusual alpha-helix stabilization afforded by charged or neutral polar residues in alanine-rich peptides. *Proc Natl Acad Sci USA* 97:13075–13079.
32. Fernández A, Berry RS (2003) Proteins with H-bond packing defects are highly interactive with lipid bilayers: Implications for amyloidogenesis. *Proc Natl Acad Sci USA* 100:2391–2396.